

A Semi-analytical Method for Channel Modeling in Diffusion-based Molecular Communication Networks

Mohammad Zoofaghari, Hamidreza Arjmandi, Ali Etemadi, Ilangko Balasingham,

Abstract—Channel modeling is a challenging vital step towards the development of diffusion-based molecular communication networks (DMCNs). Analytical approaches for diffusion channel modeling are limited to simple and specific geometries and boundary conditions. Also, simulation- and experiment-driven methods are very time-consuming and computationally complex. In this paper, the channel model for DMCN employing the fundamental concentration Green's function (CGF) is characterized. A general homogeneous boundary condition framework is considered that includes any linear reaction systems at the boundaries in the environment. To obtain the CGF for a general DMCN including multiple transmitters, receivers, and other objects with arbitrary geometries and boundary conditions, a semi-analytical method (SAM) is proposed. The CGF linear integral equation (CLIE) is analytically derived. By employing the numerical method of moments, the problem of CGF derivation from CLIE is transformed into an inverse matrix problem. Moreover, a sequential SAM is proposed that converts the inversion problem of a large matrix into multiple smaller matrices reducing the computational complexity. Particle-based simulator confirms the results obtained from the proposed SAM. The convergence and run time for the proposed method are examined. Further, the error probability of a simple diffusion-based molecular communication system is analyzed and examined using the proposed method.

I. INTRODUCTION

Diffusion-based molecular communication (DMC) is a promising approach for realizing nanonetworks for various applications, e.g., healthcare applications [1]-[3]. In diffusion-based molecular communication networks (DMCNs), molecules are used to carry information from transmitter(s) to receiver(s) via a diffusion channel [4]-[5]. Modeling diffusion channels is a vital challenging prerequisite step for analyzing, designing, and implementing a DMCN that may include multiple transmitters, receivers, or other objects

Part of this paper has been presented in the Sixth Annual ACM International Conference on Nanoscale Computing and Communication, September 2019, titled by "Characterization of Diffusive Molecular Channels based on Green's Second Identity". Manuscript received September 10, 2020; revised January 19 and February 24, 2021; accepted March 5, 2021. The editor coordinating the review of this manuscript and approving it for publication was Dr. Miaowen Wen. (Corresponding author: Hamidreza Arjmandi.)

M. Zoofaghari and H. Arjmandi are with the Electrical Engineering Department, Yazd University, Yazd, 89195-741, Iran (e-mails: zoofaghari@yazd.ac.ir, arjmandi@yazd.ac.ir).

A. Etemadi is with the School of Electrical and Computer Engineering, Tarbiat Modares University, Tehran, Iran (e-mail: ali.etemadi@modares.ac.ir).

I. Balasingham is with the Intervention Center, Oslo University Hospital (OUS), 0372 Oslo, Norway, and also with the Department of Electronics and Telecommunications, Norwegian University of Science and Technology (NTNU), 7491 Trondheim, Norway (e-mail: ilangko.balasingham@ntnu.no).

with arbitrary geometries and boundary conditions. In the MC literature, three general approaches have been employed to characterize the diffusion channel: analytical approaches, simulation- and experiment-driven approaches [6].

To derive analytical models, the authors consider various simplifying assumptions about the geometry, reactions, and boundary conditions for the diffusion environment. Unbounded diffusion channel has been characterized based on a variety of assumptions, e.g., the point source transmitter, transparent spherical receiver, or the receiver covered by ligand-receptor proteins, in the presence of medium flow and/or degradation reaction [4]-[14]. Inspired by the geometry of specific entities in the body, ideal cylindrical and spherical diffusion channels (environments) have been adopted for DMC systems. In particular, a DMC system in a cylindrical environment has been considered and characterized inspired by the blood vessels and also microfluid channels [15]-[21]. Also, the diffusion channel in a spherical environment has been analyzed in [22]-[24].

In the absence of analytical models, simulation- and experiment-driven approaches can be employed to characterize the diffusion channel. Based on the scale of the details provided, the simulation-driven approaches are categorized into classes of continuum, mesoscopic, microscopic, and molecular dynamics simulations [6]. The microscopic approach has been the most common simulation method within the MC research community in which the discretized time and continuous space is employed [25]-[28]. Motivated by real-world measurement data, experiment-driven approaches may be preferred. The experiment-driven approaches are generally based on the adoption of an appropriate parametric model and optimizing the corresponding parameters to fit the measurement data [6]. Several experimentally-driven testbeds have been introduced for modeling both biological [29]-[31] and non-biological [32]-[33] systems.

The analytical methods are restricted to the specific symmetrical geometries with simplifying assumptions. Moreover, the analytical derivations may not be extendable when the considered environment changes partially, e.g., by including new transmitters, receivers, or obstacles. On the other hand, simulation-driven approaches are computationally complex, time-consuming, and non-reusable. Also, experiment-driven approaches are usually expensive and difficult to implement. This motivates the development of a semi-analytical approach that reduces the computational burden and increases the flexibility to consider arbitrary geometries and boundary condi-

tions.

In this paper, we propose a semi-analytical method (SAM) to characterize the diffusion channel for a DMCN including multiple transmitters, receivers, and obstacles with arbitrary geometries. A pure diffusion environment (diffusion without flow) in the presence of degradation is considered. The boundary conditions implied by the objects are assumed to be adopted arbitrarily from a general homogeneous boundary condition framework. This framework enables us to model any linearly modeled process at the boundaries e.g., irreversible and reversible first-order reactions, simplified biological processes at the cell membrane like carrier-mediated transport and transcytosis¹.

The main contributions of this paper can be summarized as follows:

- We show how the average received signal at a receiver could be a sufficient statistic for characterization of the communication channel between a pair of transmitter and receiver in the DMCN. By applying the Green's function theorem, the relation between the average received signal and the concentration Green's function (CGF) of the environment given the newly-introduced homogeneous boundary conditions is derived.
- Based on Green's second identity, we derive concentration Green's function linear integral equation (CLIE) which analytically relates the CGF value at an arbitrary point to the CGF values at the boundary points.
- To obtain the CGF values at the boundary points, we employ the method of moments that expand the unknown CGF in CLIE in terms of a set of basis functions with unknown coefficients (moments) leading to an inverse matrix problem. In the original form of this method, we use the given CGF for the unbounded environment and the unknown coefficients are obtained through the inverse matrix problem.
- Further, we propose a sequential SAM algorithm which is computationally less complex than the original form based on the Green's function for the unbounded environment.

The proposed SAM method utilizes the analytical CLIE and numerical method of moments. Compared to the simulation-driven approaches e.g., finite-difference time-domain and finite element methods, that mesh the whole space (surface and volume in 2-dimensional and 3-dimensional spaces, respectively), the proposed SAM requires only meshing the boundaries (the lines and surfaces, respectively), which is significantly less complicated. Moreover, the proposed sequential SAM method enables reuse of the Green's function of the environment when a new object e.g., transmitter, receiver, or obstacle is added to the environment. Besides, the proposed analytical CLIE can be employed to obtain CGF for special geometries in terms of closed-form expressions, as we demonstrate in a simple example. To evaluate the proposed SAM, we consider simple scenarios and obtain the CGF from the proposed SAM and Particle-based simulator (PBS). The PBS confirms the results

¹Transcytosis is referred to a type of transcellular process responsible for transporting various macromolecules across the interior of a cell.

TABLE I
SUMMARY OF THE NOTATION.

| Variable | Definition |
|---|--|
| N_b | The total number of boundaries (objects) |
| N_b^R | Number of generalized Robin's boundary conditions |
| N_b^D | Number of Dirichlet's boundary conditions |
| $\partial\mathcal{D}$ | Entire boundary of the diffusion environment |
| $\partial\mathcal{D}_i$ | The boundary of object i |
| \mathbf{L}_i and \mathbf{D}_i | Linear differential operators at boundary i |
| $\mathcal{L}_i(\omega)$ and $\mathcal{D}_i(\omega)$ | Fourier transform of \mathbf{L}_i and \mathbf{D}_i |
| D | Diffusion coefficient |
| k_d | Degradation reaction constant |
| k_f | Forward reaction constant |
| k_b | Backward reaction constant |
| k_v | Internalization constant |
| $c(\bar{r}, t)$ | Concentration function at point \bar{r} and time t as the solution of diffusion problem (5) |
| $C(\bar{r}, \omega)$ | Fourier transform of $c(\bar{r}, t)$ |
| $g(\bar{r}, t \bar{r}', t')$ | CGF for diffusion problem (14) given the point source at \bar{r}' with impulsive release at t' |
| $G(\bar{r}, \omega \bar{r}', t')$ | Fourier transform of $g(\bar{r}, t \bar{r}', t')$ |
| $h(\bar{r}, t \bar{r}', t')$ | CGF for unbounded environment given the point source at \bar{r}' with impulsive release at t' |
| $H(\bar{r}, \omega \bar{r}', t')$ | Fourier transform of $h(\bar{r}, t \bar{r}', t')$ |
| $H_i(\bar{r}, \omega \bar{r}', t')$ | Fourier transform of CGF for the environment in the presence of boundaries $\{1, 2, \dots, i\}$ |
| P_i^m | Pulse basis function over m th mesh of i th boundary |
| U_i^m | The unknown coefficient corresponding to P_i^m |
| $J_m(\cdot)$ | Bessel function of order m |
| $\mathcal{H}_m^{(2)}(\cdot)$ | Second kind Hankel function of order m |

obtained from the proposed SAM. We examine the convergence of the proposed method by defining a convergence error measure. Further, the performance of a simple diffusion-based molecular communication system is analyzed and examined in terms of error probability employing the proposed method.

The paper is organized as follows. The system model and the problem is described in Section II. The Green's function theorem is presented in Section III which leads to the derivation of the CLIE for the DMCN environment. In Section IV, the semi-analytical method is developed to numerically solve the CLIE and obtain the CGF over the surface of the incorporated boundaries. The simulation and numerical results are presented in Section V. Finally, the paper is concluded in Section VI. A summary of the notation used in this paper is given in Table I.

II. SYSTEM MODEL AND PROBLEM FORMULATION

A. Diffusion-based molecular communication networks

In DMCN, we have generally multiple transmitters and receivers nanomachines in the diffusion environment where the transmitter(s) release the molecules carrying information encoded in the concentration, type, and/or release time of the molecules. For any communication analysis, it is required to characterize the information channel in terms of the received signal at the receiver(s) given the release signal at the transmitter(s). We assume independent trajectories in the DMC environment and independent reactions at the boundaries for

different information molecules.² Given this assumption, the average concentration function of received molecules versus time could be sufficient to characterize different statistical models for the received signal at the receiver. As an example, we provide the following important model:

Example 1. Molecular Poisson Network [34]-[36]: Time is divided into equal time slots. The transmitters and receivers are assumed to be synchronized. The transmitter j , $j = 1, \dots, N_{tx}$ releases the molecules by the average rate $X_k^j(\bar{r}', t')$, $\bar{r}' \in \Omega_j$ $\text{mols}^{-1}\text{m}^{-2}$ in the environment at time slot k , where Ω_j denotes the set of boundary points of the transmitter. The number of molecules that are released at $\bar{r}' \in \Omega_j$ into the environment at time slot k can be modeled as Poisson process with rate $X_k^j(\bar{r}', t')$. From the thinning property of the Poisson distribution, the received signal at the l th receiver, time t in the time slot i ($t \in [(i-1)T, iT]$) from the transmitter j , follows a Poisson process as follows

$$Y_l^{j,i}(t) \sim \text{Poisson}\left(y_l^{j,i}(t)\right), \quad (1)$$

$$t \in [(i-1)T, iT], j = 1, \dots, N_{tx}, l = 1 \dots, N_{rx},$$

which is characterized by its average, $y_l^{j,i}(t)$, which is proportional to the average concentration of received molecules. Also, the inter-symbol interference from the transmitter j and interference from other transmitters are given as follows, respectively,

$$I_l^j(t) \sim \text{Poisson}\left(\sum_{k=0}^{i-1} y_l^{j,k}(t)\right), \quad (2)$$

$$t \in [(i-1)T, iT], j = 1, \dots, N_{tx}, l = 1 \dots, N_{rx}$$

$$I_l^m(t) \sim \text{Poisson}\left(\sum_{k=0}^i y_l^{m,k}(t)\right), \quad (3)$$

$$t \in [(i-1)T, iT], m = 1, \dots, N_{tx}, m \neq j, l = 1 \dots, N_{rx}.$$

The average concentration function of received molecules depends on the concentration of information molecules diffusing in the environment and the reception process over the receiver boundary that produces molecules at the receiver boundary. The concentration of information molecules can be obtained by solving the diffusion equation subject to the boundary conditions describing the environment. In the next subsection, we describe the diffusion environment for DMCN and formulate the problem.

B. Diffusion environment model for DMCN

Consider a continuous diffusion environment denoted by \mathcal{D} which is filled with a fluid medium facing N_b disjoint boundaries (objects). Each boundary may belong to a transmitter, a receiver, or another object (obstacle) in the environment. The i th boundary of the environment, i.e., the set of all points

²The assumption of independent trajectories holds when the intermolecular interactions are ignored, which is inherent to scenarios with a low concentration of molecules [44]. Also, the assumption of independent reactions at the boundaries occur when there are a large number of receptors over the boundary or the reaction over the boundary is very fast [24].

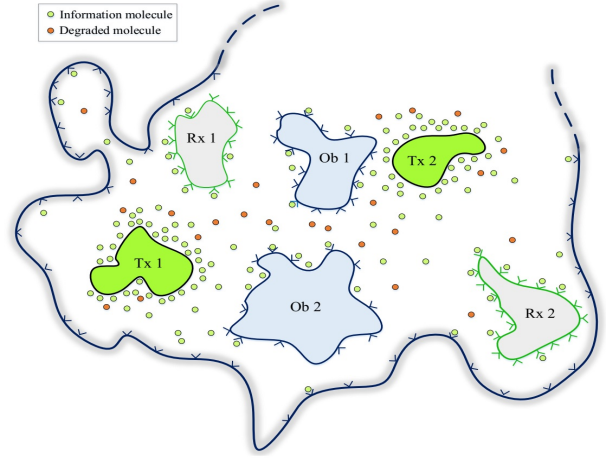


Fig. 1. Schematic diffusion environment with multiple transmitters, receivers, and obstacles of arbitrary geometries.

over the boundary of i th object, is denoted by $\partial\mathcal{D}_i$. The whole set of boundary points is denoted by $\partial\mathcal{D} = \cup_{i=1}^{N_b} \partial\mathcal{D}_i$ which represents the geometry of the environment. Obviously, $\partial\mathcal{D}$ is empty for an unbounded environment. Noteworthy, our derivations and discussions in this paper are generally presented for an environment with any number of dimensions, arbitrary geometry and shape, and are not limited to a certain coordinate system. For the sake of generality, the location of a point in the environment is denoted by a vector \bar{r} , irrespective of its dimension.

The information molecules are of type A whose diffusion coefficient in the considered fluid medium is $D \text{ m}^2 \text{ s}^{-1}$. The following degradation reaction is considered in the environment in which the (information) molecules A diffusing in the environment may be transformed to another molecule type



where k_d is the degradation reaction constant in s^{-1} . Given the molecule source with release rate per volume of $S(\bar{r}, t)$ $(\text{mol})\text{s}^{-1} \text{ m}^{-3}$ and the degradation reaction (4), the molecular diffusion is described by Fick's second law [37]

$$D\nabla^2 c(\bar{r}, t) - k_d c(\bar{r}, t) + S(\bar{r}, t) = \frac{\partial c(\bar{r}, t)}{\partial t}, \quad (5)$$

subject to the set of boundary conditions implied by the boundaries $\partial\mathcal{D}_i$, $i = 1, \dots, N_b$ where $c(\bar{r}, t)$ denotes the molecule concentration at point \bar{r} and time t .

For each i th object, irrespective of its role as a transmitter, receiver, or obstacle and considering the mutual impact between the information molecule and the boundary, *generalized Robin's boundary condition* [39] and Dirichlet boundary condition are considered

$$\mathbf{D}_i \nabla c(\bar{r}, t) \cdot \hat{n}|_{\bar{r} \in \partial\mathcal{D}_i} = \mathbf{L}_i c(\bar{r}, t) + S_b^i(\bar{r}, t), \quad i = 1, \dots, N_b^R \quad (6)$$

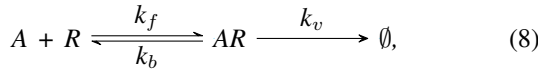
$$c(\bar{r}, t) = S_b^i(\bar{r}, t), \quad i = N_b^R + 1, \dots, N_b^R + N_b^D, \quad (7)$$

where (\cdot) denotes the inner multiplication operator, \hat{n} is the surface outward pointing normal (pointing towards the exterior

of diffusion environment) at the point $\bar{r} \in \partial\mathcal{D}_i$, \mathbf{L}_i and \mathbf{D}_i are linear differential operators, N_b^R and N_b^D denote the number of boundaries with generalized Robin's and Dirichlet boundary conditions, respectively, where $N_b^R + N_b^D = N_b$, and $S_b^i(\bar{r}, t)$ for $i \in \{1, \dots, N_b^R\}$ and $i \in \{N_b^R + 1, \dots, N_b^R + N_b^D\}$ is a source term over the i th boundary in terms of $\text{mol s}^{-1}\text{m}^{-2}$ and mol m^{-3} , respectively. Obviously, the boundaries of transmitters may have nonzero source terms.

The generalized Robin's boundary condition has been proposed in [39] that suggests a general homogeneous boundary condition framework characterizing any linearly reaction system across the object boundary by the adoption of corresponding differential operators \mathbf{L}_i and \mathbf{D}_i . In the following, we provide some special boundary conditions:

Example 2. Assume boundary $\partial\mathcal{D}$ on which the diffusing molecules A are exposed to the following chemical reaction



where k_f , k_b and k_v are forward, backward reaction constants, and internalization rate in m s^{-1} , s^{-1} , and s^{-1} , respectively. It is obvious that $k_f = 0$ corresponds to the pure reflective boundary irrespective of k_b and k_v values. Also, $k_f = \infty$ and $k_b = 0$ corresponds to the pure absorbing boundary, irrespective of k_v value. We note that this reaction approximates the main processes of carrier-mediated transport across endothelial cells at vessel walls as a first-order reaction [38], in which the molecule hitting the inner (blood-facing) membrane may bind to the carrier molecule and form carrier-target molecule compound. The compound may be internalized into the inner membrane and diffuses across the cell, breaks at the outer membrane of the cell, and releases both the target molecule and the carrier. Finally, the released carrier returns across the inner membrane.

The first-order reaction chain (8) is described by

$$\frac{\partial c(\bar{r}, t)}{\partial t} = -k_f c(\bar{r}, t) + k_b c_{AR}(\bar{r}, t), \quad \bar{r} \in \partial\mathcal{D}, \quad (9)$$

$$\frac{\partial c_{AR}(\bar{r}, t)}{\partial t} = k_f c(\bar{r}, t) - k_b c_{AR}(\bar{r}, t) - k_v c_{AR}(\bar{r}, t), \quad \bar{r} \in \partial\mathcal{D}. \quad (10)$$

Applying the differential operator of $\frac{\partial}{\partial t} + k_v$ on both sides of (9) and substituting $\frac{\partial c_{AR}(\bar{r}, t)}{\partial t} + k_v c_{AR}(\bar{r}, t)$ from (10), we obtain

$$-\left(\frac{\partial}{\partial t} + k_b + k_v\right) \frac{\partial}{\partial t} c(\bar{r}, t) = k_f \left(\frac{\partial}{\partial t} + k_v\right) c(\bar{r}, t), \quad \bar{r} \in \partial\mathcal{D}. \quad (11)$$

On the other hand, the conservation identity is implied as follows

$$\frac{\partial c(\bar{r}, t)}{\partial t} = -D\nabla c(\bar{r}, t) \cdot \hat{n}, \quad \bar{r} \in \partial\mathcal{D}. \quad (12)$$

Applying (12) to (11), we have

$$D\left(\frac{\partial}{\partial t} + k_b + k_v\right) \nabla c(\bar{r}, t) \cdot \hat{n} = k_f \left(\frac{\partial}{\partial t} + k_v\right) c(\bar{r}, t), \quad \bar{r} \in \partial\mathcal{D}. \quad (13)$$

Therefore, this boundary condition corresponds to the generalized Robin boundary condition (6) with $\mathbf{L} = k_f(\frac{\partial}{\partial t} + k_v)$ and $\mathbf{D} = D(\frac{\partial}{\partial t} + k_b + k_v)$.

The main problem is to obtain the average concentration profile of the information molecules diffusing in the described environment which is the solution of the partial differential equation (5) subject to the set of boundary conditions (6) and (7). Having this quantity, the concentration of other molecule types including the molecules produced at receivers through the boundary condition can be obtained. In the next subsection, we show how this problem reduces to the Green's function problem in this environment.

III. GREEN'S FUNCTION THEOREM

In this section, we apply Green's second identity to show that the diffusion problem for any given volume or surface molecule source is reduced to obtaining the concentration Green's function of the problem. The concentration Green's function is the response of the diffusion channel to an instantaneous point source (impulsive point source). By applying the Green's second identity, we relate the concentration function for arbitrary sources to the Green's function through a linear integral equation.

In the described environment, assume the source $S(\bar{r}, t)$ is a point source located at $\bar{r}' \in \mathcal{D}$ which has instantaneous molecule release rate of $\delta(t - t')$ molecule $(\text{mol})\text{s}^{-1}$ ($\delta(\cdot)$ is Dirac delta function). This impulsive point source is described as the function $S_{\text{im}}(\bar{r}, t, \bar{r}', t') = \delta(\bar{r} - \bar{r}')\delta(t - t')$ $\text{mol s}^{-1}\text{m}^{-3}$. For instance, this impulsive point source in the spherical coordinate system, can be represented by the function $S_{\text{im}}(\bar{r}, t, \bar{r}', t') = \frac{\delta(r-r')\delta(\theta-\theta')\delta(\varphi-\varphi')\delta(t-t')}{r^2 \sin\theta}$ $\text{mol s}^{-1}\text{m}^{-2}$, where (r, θ, φ) denote radial, elevation, and azimuth coordinates, respectively. Also, assume zero boundary sources, i.e., $S_b^i(\bar{r}, t) = 0, i = 1, \dots, N_b$.

Given the impulsive source $S_{\text{im}}(\bar{r}, t, \bar{r}', t')$ and the degradation reaction (4), and the zero boundary sources, the molecular diffusion problem would be [37]

$$D\nabla^2 g(\bar{r}, t|\bar{r}', t') - k_a g(\bar{r}, t|\bar{r}', t') + S_{\text{im}}(\bar{r}, t, \bar{r}', t') = \frac{\partial g(\bar{r}, t|\bar{r}', t')}{\partial t}, \quad (14)$$

subject to the

$$\mathbf{D}_i \nabla g(\bar{r}, t|\bar{r}', t') \cdot \hat{n}|_{\bar{r} \in \partial\mathcal{D}_i} = \mathbf{L}_i g(\bar{r}, t|\bar{r}', t'), i = 1, \dots, N_b^R \quad (15)$$

$$g(\bar{r}, t|\bar{r}', t') = 0, i = N_b^R + 1, \dots, N_b^R + N_b^D, \quad (16)$$

where $g(\bar{r}, t|\bar{r}', t')$ denotes the molecule concentration at point \bar{r} and time t and is called the concentration Green's function (CGF) of diffusion for the environment \mathcal{D} . The relation between the concentration function $c(\bar{r}, t)$ and the Green's function $g(\bar{r}, t|\bar{r}', t')$ is revealed by applying the Green's second identity in the frequency domain.

Let us define the Fourier transform of function $f(t)$ as

$$F(\omega) = \int_{-\infty}^{\infty} f(t) e^{-j\omega t} dt. \quad (17)$$

By replacing \bar{r} by \bar{r}' in (5)-(7) and taking the Fourier transform of them and also (14)-(16) in terms of t , we obtain

$$D\nabla^2 C(\bar{r}', \omega) - k_d C(\bar{r}', \omega) + S(\bar{r}', \omega) = j\omega C(\bar{r}', \omega), \quad (18)$$

$$\mathcal{D}_i \nabla C(\bar{r}', \omega) \cdot \hat{n}|_{r \in \partial \mathcal{D}_i} = \mathcal{L}_i(\omega) C(\bar{r}', \omega) + S_b^i(\bar{r}', \omega), \quad (19)$$

$$i = 1, \dots, N_b^R$$

$$C(\bar{r}', \omega) = S_b^i(\bar{r}', \omega), i = N_b^R + 1, \dots, N_b^R + N_b^D, \quad (20)$$

$$D\nabla^2 G(\bar{r}, \omega | \bar{r}', t') - k_d G(\bar{r}, \omega | \bar{r}', t') + \delta(\bar{r} - \bar{r}') e^{-j\omega t'} = j\omega G(\bar{r}, \omega | \bar{r}', t'), \quad (21)$$

$$\mathcal{D}_i(\omega) \nabla G(\bar{r}, \omega | \bar{r}', t') \cdot \hat{n}|_{r \in \partial \mathcal{D}_i} = \mathcal{L}_i(\omega) G(\bar{r}, \omega | \bar{r}', t'), \quad (22)$$

$$i = 1, \dots, N_b^R$$

$$G(\bar{r}, \omega | \bar{r}', t') = 0, \quad i = N_b^R + 1, \dots, N_b^R + N_b^D, \quad (23)$$

where $C(\bar{r}', \omega)$, $G(\bar{r}, \omega | \bar{r}', t')$, $\mathcal{L}_i(\omega)$ and $\mathcal{D}_i(\omega)$ denote the Fourier transforms of $c(\bar{r}', t)$, $g(\bar{r}, t | \bar{r}', t')$, and differential operators \mathbf{L}_i and \mathbf{D}_i , respectively.

By considering N_b infinitely thin cuts, the boundaries $\partial \mathcal{D}_i, i = 1, \dots, N_b$ can be connected together and form a closed boundary denoted by $\partial \mathcal{D}$. Considering that $C(\bar{r}', \omega)$ and $G(\bar{r}, \omega | \bar{r}', t')$ are both twice continuously differentiable functions on \mathcal{D} , the Green's second identity [41] holds and we can write

$$\int_{\mathcal{D}} (G\nabla^2 C - C\nabla^2 G) dV' = \oint_{\partial \mathcal{D}} (G\nabla C \cdot \hat{n} - C\nabla G \cdot \hat{n}) dS', \quad (24)$$

in which C and G shortly denote $C(\bar{r}', \omega)$ and $G(\bar{r}, \omega | \bar{r}', t')$, $\int_{\mathcal{D}}$ and $\oint_{\partial \mathcal{D}}$ represent the volume and surface integrals over \mathcal{D} and the closed boundary (path) $\partial \mathcal{D}$, respectively, and \hat{n} is the outward pointing normal to the surface element dS over the boundary. The right-hand side integral over the entire boundary $\partial \mathcal{D}$ can be written as the sum of the closed integrals over the boundaries $\partial \mathcal{D}_i, i = 1, \dots, N_b$ and integrals over the cuts between them. The integrals over the cuts tend to zero for infinitely thin cuts and we are left with the integrals over $\partial \mathcal{D}_i, i = 1, \dots, N_b$. Thereby, (24) can be rewritten as

$$\int_{\mathcal{D}} (G\nabla^2 C - C\nabla^2 G) dV' = \sum_{i=1}^{N_b} \oint_{\partial \mathcal{D}_i} (G\nabla C \cdot \hat{n} - C\nabla G \cdot \hat{n}) dS'. \quad (25)$$

Also, by breaking the series into two series over N_b^R generalized Robin's boundaries and N_b^D Dirichlet boundaries, we rewrite (25) as (26) at the top of the next page. Now, by substituting $\nabla^2 C$ and $\nabla^2 G$ from (18) and (21) in the left side, $\nabla C \cdot \hat{n}$ and $\nabla G \cdot \hat{n}$ from (19) and (22) in the first term of the right side, and C and G from (20) and (23) in the second term of the right side, respectively, applying some simple manipulations, (26) reduces to the linear integral equation (27) at the top of the next page. Therefore, the diffusion problem for any given volume or surface molecule source is reduced to obtain the Green's function of the problem.

Obtaining the Green's function in a closed-form expression is very challenging, but possible for some symmetric geometries (boundaries) [21], [24]. In the next section, we provide the method of moments approach to obtain the Green's function numerically in which the diffusion problem reduces to a linear system of equations with unknown variables as coefficients of a set of basis functions.

IV. SEMI-ANALYTICAL METHOD

Suppose that $g(\bar{r}, t | \bar{r}_0, t_0)$ denotes the CGF for diffusion in the environment \mathcal{D} , i.e., the concentration of information molecules at \bar{r} and time t given the impulsive point source $S(\bar{r}, t, \bar{r}_0, t_0) = \delta(\bar{r} - \bar{r}_0)\delta(t - t_0)$ mol s⁻¹ m⁻³, that satisfies the time domain diffusion equation (14) subject to the boundary conditions (15)-(16) and corresponding frequency domain equation (21) subject to the (22)-(23). In the following, we relate the frequency domain CGF of G satisfying (21) given the boundary conditions (22)-(23) to the known CGF of the unbounded environment (the environment without any boundaries) by employing the Green's second identity leading to a linear integral equation.

Now, consider the diffusion equations for the unbounded environment given impulsive point source $S(\bar{r}, t, \bar{r}', t') = \delta(\bar{r} - \bar{r}')\delta(t - t')$ in the time and frequency domains, respectively, as follows

$$D\nabla^2 h(\bar{r}, t | \bar{r}', t') - k_d h(\bar{r}, t | \bar{r}', t') + \delta(\bar{r} - \bar{r}')\delta(t - t') = \frac{\partial h(\bar{r}, t | \bar{r}', t')}{\partial t}, \quad (28)$$

$$D\nabla^2 H(\bar{r}, \omega | \bar{r}', t') - k_d H(\bar{r}, \omega | \bar{r}', t') + \delta(\bar{r} - \bar{r}')e^{-j\omega t'} = j\omega H(\bar{r}, \omega | \bar{r}', t'). \quad (29)$$

Considering that $G(\bar{r}, \omega | \bar{r}_0, t_0)$ and $H(\bar{r}, \omega | \bar{r}', t')$ are both twice continuously differentiable functions on \mathcal{D} , the Green's second identity [41] holds and we can write

$$\int_{\mathcal{D}} (H\nabla^2 G - G\nabla^2 H) dV = \oint_{\partial \mathcal{D}} (H\nabla G \cdot \hat{n} - G\nabla H \cdot \hat{n}) dS, \quad (30)$$

in which G and H shortly denote $G(\bar{r}, \omega | \bar{r}_0, t_0)$ and $H(\bar{r}, \omega | \bar{r}', t')$, $\int_{\mathcal{D}}$ and $\oint_{\partial \mathcal{D}}$ represent the volume and surface integrals over \mathcal{D} and the closed boundary (path) $\partial \mathcal{D}$, respectively, and \hat{n} is the outward pointing normal to the surface element dS over the boundary.

Similar to (26), we can break the integral at the right side into individual boundaries and obtain (31) at the top of the next page.

Now, by substituting $\nabla^2 G$ and $\nabla^2 H$ from (21) and (29) in the left side, $\nabla G \cdot \hat{n}$ from (22) in the first term of the right side, and $G = 0$ from (23) in the second term of the right side, respectively, applying some simple manipulations, (31) reduces to the linear integral equation in (32) at the top of the next page in which $\gamma = 1$ and $\frac{1}{2}$ for $\bar{r}' \notin \partial \mathcal{D}$ and $\bar{r}' \in \partial \mathcal{D}$, respectively. We note that the coefficient $\gamma = \frac{1}{2}$ appears for

$$\int_{\mathcal{D}} (G\nabla^2 C - C\nabla^2 G) dV' = \sum_{i=1}^{N_b^R} \oint_{\partial\mathcal{D}_i} (G\nabla C \cdot \hat{n} - C\nabla G \cdot \hat{n}) dS' + \sum_{i=N_b^R+1}^{N_b} \oint_{\partial\mathcal{D}_i} (G\nabla C \cdot \hat{n} - C\nabla G \cdot \hat{n}) dS'. \quad (26)$$

$$C(\bar{r}, \omega) e^{-j\omega t'} = \int_{\mathcal{D}} G(\bar{r}, \omega | \bar{r}', t') S(\bar{r}', \omega) dV' + \sum_{i=1}^{N_b^R} \oint_{\partial\mathcal{D}_i} G(\bar{r}, \omega | \bar{r}', t') S_b^i(\bar{r}', \omega) dS' - \sum_{i=N_b^R+1}^{N_b} \oint_{\partial\mathcal{D}_i} S_b^i(\bar{r}', \omega) \nabla G \cdot \hat{n} dS'. \quad (27)$$

$$\int_{\mathcal{D}} (H\nabla^2 G - G\nabla^2 H) dV = \sum_{i=1}^{N_b^R} \oint_{\partial\mathcal{D}_i} (H\nabla G \cdot \hat{n} - G\nabla H \cdot \hat{n}) + \sum_{i=N_b^R+1}^{N_b} \oint_{\partial\mathcal{D}_i} (H\nabla G \cdot \hat{n} - G\nabla H \cdot \hat{n}) dS. \quad (31)$$

$$\begin{aligned} H(\bar{r}_0, \omega | \bar{r}', t') e^{-j\omega t_0} - \gamma G(\bar{r}', \omega | \bar{r}_0, t_0) e^{-j\omega t'} = \\ \sum_{i=1}^{N_b^R} \oint_{\partial\mathcal{D}_i} G(\bar{r}, \omega | \bar{r}_0, t_0) (H(\bar{r}, \omega | \bar{r}', t') (\frac{D\mathcal{L}_i(\omega)}{D_i(\omega)} - \nabla H(\bar{r}, \omega | \bar{r}', t') \cdot \hat{n}) dS + \sum_{i=N_b^R+1}^{N_b} \oint_{\partial\mathcal{D}_i} (DH(\bar{r}, \omega | \bar{r}', t') \nabla G(\bar{r}, \omega | \bar{r}_0, t_0) \cdot \hat{n}) dS, \end{aligned} \quad (32)$$

$\bar{r}' \in \partial\mathcal{D}$ since the concentration of molecules at one side (inside) of the boundary is zero and then we have

$$\int_{\mathcal{D}} G(\bar{r}, \omega | \bar{r}_0, t_0) \delta(\bar{r} - \bar{r}') dV = \frac{1}{2}, \quad (33)$$

for $\bar{r}' \in \partial\mathcal{D}$.

Eq. (32) is a second kind Fredholm integral equation [41] and we refer to as *concentration Green's function integral equation (CLIE)*.

Corollary 1. *The CLIE suggests that the CGF at arbitrary observation point $r' \in \mathcal{D}$, i.e., $G(\bar{r}', \omega | \bar{r}_0, t_0)$ only depends on the CGF and its gradient over the boundaries linearly, i.e.,*

$$G(\bar{r}, \omega | \bar{r}_0, t_0), r \in \partial\mathcal{D}_i, i = 1, \dots, N_b^R \quad (34)$$

$$\nabla G(\bar{r}, \omega | \bar{r}_0, t_0), r \in \partial\mathcal{D}_i, i = N_b^R + 1, \dots, N_b. \quad (35)$$

In the next subsection, the numerical method of moments is proposed to obtain these values at the boundaries. This method can be employed for arbitrary geometries of environment. However, for some special geometries, CLIE can be employed to obtain CGF in terms of closed-form expressions by considering right choice of basis functions to represent the Green's function. In the following example, we obtain the closed-form expression for CGF in a simple 2-dimensional circular environment.

Example 3. *Assume a circular environment with radius a and Robin's boundary condition given in (6). The polar coordinate system is considered in which (r, φ) represent the radial and azimuthal components of point location, respectively. The integral $\oint dS$ in (32) reduces to a line integral $\int_0^{2\pi} (\cdot) d\varphi$ over the circular boundary. To derive CGF in the circular environment for an arbitrary point \bar{r}' , $G(\bar{r}', \omega | \bar{r}_0, t_0)$ from (32), one needs to have the CGF at the boundary points $G(\bar{r}, \omega | \bar{r}_0, t_0)$, $\bar{r} \in \partial\mathcal{D}$, i.e., $\bar{r} = a\hat{r}$ where \hat{r} is the radial unit*

vector in the polar coordinate system. To obtain $G(\bar{r}, \omega | \bar{r}_0, t_0)$, $\bar{r} \in \partial\mathcal{D}$, the following series representation is employed

$$G(a\hat{r}, \omega | \bar{r}_0, t_0) = \sum_{m=-\infty}^{\infty} g_m e^{jm\varphi}, \quad (36)$$

where,

$$g_m = \frac{1}{2\pi} \int_0^{2\pi} G(a\hat{r}, \omega | \bar{r}_0, t_0) e^{-jm\varphi} d\varphi. \quad (37)$$

As the solution of (29), CGF for unbounded environment is given by

$$H(\bar{r}, \omega | \bar{r}', t') = \frac{-j}{4D} H_0^{(2)}(Q|r - r'|) e^{-j\omega t'}, \quad (38)$$

in which $Q = \sqrt{-j\omega/D}$. The series representations for $H(a\hat{r}, \omega | \bar{r}')$ in (38) and its gradient, $\nabla H(a\hat{r}, \omega | \bar{r}') \cdot \hat{n}$, are obtained as (39) and (40) at the top of the next page, respectively, where $J_m(\cdot)$ and $\mathcal{H}_m^{(2)}(\cdot)$ are the Bessel and the second kind Hankel functions of order m , respectively. Considering (32) for the point \bar{r}' over the boundary, substituting $H(a\hat{r}, \omega | \bar{r}')$ and $\nabla H(a\hat{r}, \omega | \bar{r}') \cdot \hat{n}$ from (39)-(40), applying (36)-(37), and manipulating the two series in both sides of (32), lead to a closed-form expression for g_m given by (41) at the top of the next page. For an arbitrary observation point \bar{r} , utilizing (36) in (32) yields the following expression for CGF in frequency domain

$$\begin{aligned} G(r\hat{r}, \omega | \bar{r}_0, t_0) = \sum_{m=-\infty}^{\infty} -g_m \mathcal{H}_m^{(2)}(Qr) e^{-jm\varphi} \\ \left(\frac{-j}{4D} J_m(Qa) \mathcal{L}(\omega) + \frac{jQ}{8D} (J_{m-1}(Qa) - J_{m+1}(Qa)) \right) \\ + \frac{-j}{4D} \mathcal{H}_0^{(2)}(Q|\bar{r} - \bar{r}_0|). \end{aligned} \quad (42)$$

Remark 1. *Of note, the concentration of ligand-receptor complexes over the boundary in Example*

$$H(a\hat{r}, \omega | \bar{r}', t') = \frac{-j}{4D} \mathcal{H}_0^{(2)}(Q|a\hat{r} - r'\hat{r}') e^{-j\omega t'} = \frac{-j}{4D} \sum_{m=-\infty}^{\infty} J_m(Qa) \mathcal{H}_m^{(2)}(Qr') e^{jm(\varphi' - \varphi)} e^{-j\omega t'}, \quad (39)$$

$$\nabla H(a\hat{r}, \omega | \bar{r}', t') \cdot \hat{n} = \frac{-jQ}{8D} \sum_{m=-\infty}^{\infty} \mathcal{H}_m^2(Qr') (J_{m-1}(Qa) - J_{m+1}(Qa)) e^{jm(\varphi' - \varphi)} e^{-j\omega t'}, \quad (40)$$

$$g_m = \frac{\frac{-j}{4D} \mathcal{H}_m^{(2)}(Qr_0) J_m(Qa) e^{jm\varphi_0}}{\gamma + 2\pi a \left(\frac{-j}{4D} J_m(Qa) \mathcal{H}_m^{(2)}(Qa) \mathcal{L}(\omega) - \frac{-jQ}{8D} (\mathcal{H}_m^{(2)}(Qa) (J_{m-1}(Qa) - J_{m+1}(Qa))) \right)}. \quad (41)$$

2, $c_{\text{AR}_i}(\bar{r}, t | \bar{r}_0, t_0)|_{r \in \partial \mathcal{D}_i}$, can be obtained given the concentration of information molecules A over the boundary from (10) in frequency domain

$$C_{\text{AR}_i}(\bar{r}, \omega | \bar{r}_0, t_0)|_{r \in \partial \mathcal{D}_i} = \frac{k_f}{j\omega + k_b + k_v} C(\bar{r}, \omega | \bar{r}_0, t_0). \quad (43)$$

A. Obtaining unknown functions using method of moments

In this section, we employ the method of moments to obtain the unknown functions, i.e., $G(\bar{r}, \omega | \bar{r}_0, t_0)$ and $\nabla G(\bar{r}, \omega | \bar{r}_0, t_0)$, $\bar{r} \in \mathcal{D}_i$ for a given ω in (32). The method of moments expands the unknown functions in terms of a set of basis functions with unknown coefficients (moments). Applying this expansion to the CLIE (32) and adoption of enough number of matching points of \bar{r}' , we obtain a system of linear equations of the unknown coefficients.

In CLIE given in (32), we define

$$B(\bar{r}') = H(\bar{r}_0, \omega | \bar{r}', t') e^{-j\omega t_0} - \gamma G(\bar{r}', \omega | \bar{r}_0, t_0) e^{-j\omega t'}, \quad (44)$$

$$U_i(\bar{r}) = G(\bar{r}, \omega | \bar{r}_0, t_0), \quad \bar{r} \in \mathcal{D}_i, i = 1, \dots, N_b^R \quad (45)$$

$$U_i(\bar{r}) = \nabla G(\bar{r}, \omega | \bar{r}_0, t_0), \quad \bar{r} \in \mathcal{D}_i, i = N_b^R + 1, \dots, N_b, \quad (46)$$

and

$$K_i(\bar{r}, \bar{r}') = H(\bar{r}, \omega | \bar{r}', t') \left(\frac{D\mathcal{L}_i(\omega)}{\mathcal{D}_i(\omega)} - \nabla H(\bar{r}, \omega | \bar{r}', t') \cdot \hat{n} \right), \quad (47)$$

$$r \in \mathcal{D}_i, i = 1, \dots, N_b^R$$

$$K_i(\bar{r}, \bar{r}') = DH(\bar{r}, \omega | \bar{r}', t'), r \in \mathcal{D}_i, i = N_b^R + 1, \dots, N_b \quad (48)$$

Therefore, (32) can be written as

$$B(\bar{r}') = \sum_{i=1}^{N_b} \oint_{\partial \mathcal{D}_i} K_i(\bar{r}, \bar{r}') U_i(\bar{r}) dS. \quad (49)$$

Each boundary $\partial \mathcal{D}_i$ is discretized (meshed) into M_i sub-boundaries called *meshes* $\partial \mathcal{D}_i^m$, $m = 1, \dots, M_i$ whose areas are denoted by ΔS_i^m , $m = 1, \dots, M_i$. For sufficiently large number of meshes (i.e., a sufficiently small areas of sub-boundaries), $U_i(\bar{r})$ is approximately constant at each mesh $\partial \mathcal{D}_i^m$. Thus, each mesh $\partial \mathcal{D}_i^m$, $m = 1, \dots, M_i$ is represented by point $\bar{r}_i^m \in \partial \mathcal{D}_i$ and $U_i(\bar{r})$ value at the mesh $\partial \mathcal{D}_i^m$ is

denoted by $U_i(\bar{r}_i^m) = U_i^m$. Therefore, $U_i(\bar{r})$ can be expanded in terms of pulse basis functions as follows:

$$U_i(\bar{r}) = \sum_{m=1}^{M_i} U_i^m P_i^m(\bar{r}), \quad \bar{r} \in \mathcal{D}_i, \quad (50)$$

where P_i^m is the pulse basis function given by

$$P_i^m(\bar{r}) = \begin{cases} 1 & \bar{r} \in \partial \mathcal{D}_i^m \\ 0 & \bar{r} \notin \partial \mathcal{D}_i^m \end{cases} \quad (51)$$

Substituting $U_i(\bar{r})$ from (50), (49) is given by

$$B(\bar{r}') = \sum_{i=1}^{N_b} \sum_{m=1}^{M_i} U_i^m \int_{\partial \mathcal{D}_i^m} K_i(\bar{r}, \bar{r}') dS. \quad (52)$$

where U_i^m denotes the pulse function amplitude over the m th mesh in the i th boundary. The integral in 52 can be approximated by various quadrature rules like rectangular, trapezoidal, Simpson's and etc.

Based on (52), $B(\bar{r}')$ and correspondingly $G(\bar{r}', \omega | \bar{r}_0, t_0)$ at arbitrary observation point $\bar{r}' \in \mathcal{D}$ can be computed, if the coefficients U_i^m for all $i = 1, \dots, N_b$ and $m = 1, \dots, M_i$ are known. To obtain the unknown coefficients U_i^m for all $i = 1, \dots, N_b$ and $m = 1, \dots, M_i$, we can constitute independent linear equations by matching the two sides of (52) at enough number of observation points or test points \bar{r}' which is called point matching technique.

To this end, we adopt $\sum_{i=1}^{N_b} M_i$ test points representing the meshes, i.e., \bar{r}_q^l , $q = 1, \dots, N_b$ and $l = 1, \dots, M_q$, where $G(\bar{r}_q^l, \omega | \bar{r}_0, t_0)$ and $\nabla G(\bar{r}_q^l, \omega | \bar{r}_0, t_0)$ are (matches) our unknown coefficients $U_q(r_q^l) = U_q^l$ for $q = 1, \dots, N_b^R$ and $q = N_b^R + 1, \dots, N_b$, respectively. For each test point \bar{r}_q^l , $q = 1, \dots, N_b$ and $l = 1, \dots, M_q$, we obtain the following linear equation

$$\tilde{B}(\bar{r}_q^l) = \sum_{i=1}^{N_b} \sum_{m=1}^{M_i} U_i^m \int_{\partial \mathcal{D}_i^m} K_i(\bar{r}, \bar{r}_q^l) dS + \frac{1}{2} U_q^l e^{-j\omega t'}, \quad (53)$$

$$q = 1, \dots, N_b, \quad l = 1, \dots, M_q,$$

where $\tilde{B}(\bar{r}_q^l) = H(\bar{r}_0, \omega | \bar{r}_q^l, t') e^{-j\omega t_0}$. We note that

$$U_q^l = 0, \quad \bar{r} \in \mathcal{D}_i, q = N_b^R + 1, \dots, N_b, \quad (54)$$

since the Green's function over the Dirichlet boundaries is zero, i.e., $G(\bar{r}, \omega | \bar{r}_0, t_0) = 0$ for $\bar{r} \in \mathcal{D}_i$ as (23) implies. The

matrix form of this linear equation system can be written as follows

$$[\tilde{B}] = \left([\tilde{K}] + \frac{1}{2}[I]e^{-j\omega t'} \right) [U], \quad (55)$$

where $[\tilde{B}]$ and $[U]$ are vectors of length $\sum_{i=1}^{N_b} M_i$ whose $(\sum_{x=1}^{q-1} M_x + l - 1)$ th elements are $\tilde{B}(r_q^l)$ and U_q^l , respectively, $[\tilde{K}]$ is a $\sum_{i=1}^{N_b} M_i \times \sum_{i=1}^{N_b} M_i$ matrix whose $((\sum_{x=1}^{i-1} M_x + m - 1), (\sum_{x=1}^{q-1} M_x + l - 1))$ th element is $\int_{\partial\mathcal{D}_i} K(r, r_q^l) dS$ and $[I]$ is identity matrix of size $\sum_{i=1}^{N_b} M_i$.

By solving the linear system of equations in (55), the unknown coefficients U_i^m are obtained. Having the unknown coefficients U_i^m , the Fourier transform $G(\bar{r}', \omega | \bar{r}_0, t_0)$ can be computed based on (32), for arbitrary observation point \bar{r}' for each ω , given \bar{r}_0 and t_0 . Obtaining $C(\bar{r}', \omega | \bar{r}_0, t_0)$ for all ω and taking numerical Fourier transform inverse, the time domain concentration $g(\bar{r}', t | \bar{r}_0, t_0)$ is resulted.

Example 4. Assume two objects ($N_b = 2$) in a 2-D unbounded environment where each boundary is divided into two sub-boundaries ($M_1 = 1, M_2 = 1$). The \bar{r}_1^1 and \bar{r}_2^1 represent the meshes of objects 1 and 2, respectively, and the corresponding surface areas are denoted by ΔS_1^1 and ΔS_2^1 , respectively. Assuming the objects 1 and 2 have generalized Robin's and Dirichlet boundary conditions, respectively, (55) can be written as (56) at the top of the next page.

Definition 1. Without loss of generality, we adopt $t' = 0$ and define $[\mathcal{K}] = [\tilde{K}] + \frac{1}{2}[I]$ as the **diffusion characteristic matrix (DCM)** for the considered environment which depends on the Green's function of the unbounded environment and the geometry of the environment and independent of the source location.

The DCM is independent of the source location. Thereby, to obtain the unknown coefficients $[U]$ given any arbitrary impulsive source $\delta(\bar{r} - \bar{r}_0)\delta(t - t_0)$, the inversion of the DCM does not need to be repeated.

Remark 2. The proposed SAM method utilizes both the analytical and the numerical parts. The analytical CLIE part relates the CGF value at an arbitrary point to the CGF values at the boundary points. Thereby, the complexity from n -dimensional diffusion environment reduces to the $(n-1)$ -dimensional boundaries. This makes the method significantly less complicated compared to the simulation-driven approaches that mesh the n -dimensional diffusion space. On the other hand, the numerical method of moments provide flexibility to take into account the arbitrary geometries and number of objects in the DMCN.

B. Sequential semi-analytical method

In this subsection, we propose a sequential (step-by-step) algorithm to obtain the Green's function which is less computationally complex than obtaining the Green's function in one step using the Green's function for the unbounded environment. To this end, we consider the inclusion of only one boundary to the environment in each iteration until all the boundaries are included. In this way, the large size matrix

inverse problem in (56) reduces to multiple small size matrices which have lower computational complexity.

We consider a primary environment with some boundaries with known Green's function rather than the unbounded diffusion environment considered in the previous subsection. Consider diffusion environment denoted by \mathcal{D} with some boundaries (or obstacles) whose set of all points, is denoted by $\partial\mathcal{D}$. Obviously, $\partial\mathcal{D}$ is empty for an unbounded environment. Assume the Green's function for this primary environment is given by $h(\bar{r}, t | \bar{r}', t')$ which satisfies (28) given its boundary conditions on $\partial\mathcal{D}$.

Assume $H_0(\bar{r}, \omega | \bar{r}', t')$ is the Green's function for the unbounded environment we denote by $E = 0$. In the first iteration $i = 1$, we consider the boundary $i = 1$ is added to the environment $E = 0$ and form the environment $E = 1$ in iteration $i = 1$. Then, we constitute the matrix $[\mathcal{K}]$ and compute its inverse which characterize the CGF for the environment $E = 1$ in iteration $i = 1$ and provides the CGF values over the meshes of boundary $i = 1$ based on (56). Thereby, the CGF in the environment $E = 1$ at each arbitrary observation point, $H_1(\bar{r}, \omega | \bar{r}', t')$, can be obtained as linear combination of the CGF values over the boundary $i = 1$. In the iteration 2, the boundary $i = 2$ is added to the environment $E = 1$ to form $E = 2$. The CGF for $E = 2$, $H_2(\bar{r}, \omega | \bar{r}', t')$, is obtained based on known CGF $H_1(\bar{r}, \omega | \bar{r}', t')$. The algorithm continues until all the N_b boundaries are included. Algorithm 1 represents this sequential algorithm.

Algorithm 1 Sequential SAM

Require: Set iteration number $i = 0$ and $E = 0$ as the unbounded environment $\mathcal{D}_0 = \emptyset$ with CGF $H_0(\bar{r}, \omega | \bar{r}', t')$,

- 1: **while** $i < N_b$ **do**
- 2: $i = i + 1$,
- 3: Consider environment $E = i$ by including the boundary i , \mathcal{D}_i , to the $E = i - 1$: $\mathcal{D}_i = \partial\mathcal{D}_{i-1} \cup \mathcal{D}_i$,
- 4: Constitute the matrix $[\mathcal{K}]$ and invert it,
- 5: Constitute the vector $[\tilde{B}]$ by using the CGF $H_{i-1}(\bar{r}, \omega | \bar{r}', t')$,
- 6: Compute the CGF over the meshes of the included boundary $U_i^m, m = 1, \dots, M_i$ which characterize $H_i(\bar{r}, \omega | \bar{r}', t')$.
- 7: **end while**

Using this algorithm, the computational complexity significantly decreases. Let us clarify this with an example. Assume we have meshed N_b boundaries each with M meshes. Obtaining the CGF in one step needs the inverse of the DCM of size (the number of columns (rows)) ($N_b \times M$) whose complexity is of order $O(N_b^3 M^3)$ by Gauss–Jordan elimination algorithm. But, if we obtain the CGF in N_b iterations, we have broken the problem into N_b inversion of DCM of size M where the complexity is of order $O(N_b M^3)$.

Remark 3. The first step of the algorithm ($i = 0$) may start from a bounded environment with closed-form expression for its CGF. For instance, assume the transmitter(s), receiver(s), and obstacles are in a tube-like environment whose CGF is known [21]. Thereby, one can start the algorithm from this

$$\begin{aligned} & \left[\frac{H(\bar{r}_0, \omega | \bar{r}_1^1, t') e^{-j\omega t_0}}{H(\bar{r}_0, \omega | \bar{r}_2^1, t') e^{-j\omega t_0}} \right] = \\ & \left[\begin{array}{cc} H(\bar{r}_1^1, \omega | \bar{r}_1^1, t') (\mathcal{L}_i(\omega) - \nabla H(\bar{r}_1^1, \omega | \bar{r}_1^1, t') \cdot \hat{n}) \Delta S_1^1 & H(\bar{r}_2^1, \omega | \bar{r}_1^1, t') (\mathcal{L}_i(\omega) - \nabla H(\bar{r}_2^1, \omega | \bar{r}_1^1, t') \cdot \hat{n}) \Delta S_2^1 \\ H(\bar{r}_1^1, \omega | \bar{r}_2^1, t') (\mathcal{L}_i(\omega) - \nabla H(\bar{r}_1^1, \omega | \bar{r}_2^1, t') \cdot \hat{n}) \Delta S_1^1 & H(\bar{r}_2^1, \omega | \bar{r}_2^1, t') (\mathcal{L}_i(\omega) - \nabla H(\bar{r}_2^1, \omega | \bar{r}_2^1, t') \cdot \hat{n}) \Delta S_2^1 \end{array} \right] \left[\begin{array}{c} G(\bar{r}_1^1, \omega | \bar{r}_0, t_0) \\ \nabla G(\bar{r}_2^1, \omega | \bar{r}_0, t_0) \end{array} \right] \end{aligned} \quad (56)$$

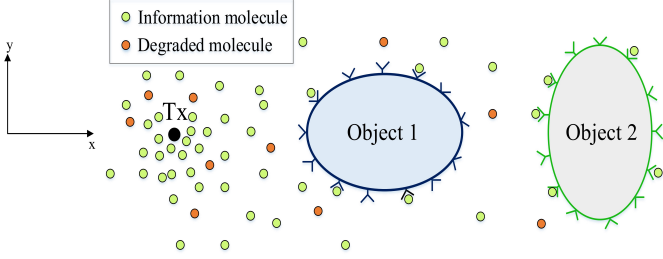


Fig. 2. 2-dimensional diffusion environment with two elliptical objects (receiver or obstacle) in the environment.

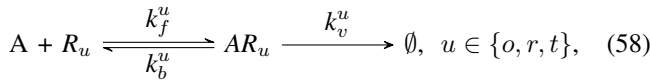
bounded environment and include other boundaries step-by-step.

V. SIMULATION AND NUMERICAL RESULTS

As a proof of concept, we consider a diffusive molecular communication system in 2-dimensional diffusion environment described in a Cartesian coordinate system where (x, y) denotes the location of a specific point along the x -axis and y -axis, respectively. Two elliptical objects are assumed in the environment whose boundary points are given by all (x, y) satisfying

$$\frac{(x - x_u)^2}{b_u^2} + \frac{(y - y_u)^2}{a_u^2} = 1, \quad u \in \{o, r, t\}, \quad (57)$$

where (x_u, y_u) , a_u , and b_u denote the center and the length of semi-major and semi-minor axes of ellipse, respectively. Each object may play the role of obstacle (o), receiver (r) or transmitter (t) in different scenarios. Each boundary is fully covered by the receptor proteins described in Example 2 characterized by



We remark that the proposed results obtained in this paper are independent of the number of dimensions and objects, and the shape of objects. Hence, 2-dimensional environment is leveraged as a proof of concept in this paper. For 3-dimensional environment, the boundaries are surfaces that require a more complex meshing compared to meshing for line boundaries in 2-dimensional environment. Although, the SAM has been proposed for any homogeneous boundary conditions, we considered (58) for results section in this paper, which is able to model some important types of boundaries including reflective, fully absorbing, partially absorbing and internalization processes, depending on the parameter values. The diffusion coefficient of the information molecule A is assumed $D = 10^{-9} \text{ m}^2 \text{ s}^{-1}$.

The rest of this section is organized as follows. We elaborate the implementation of the proposed SAM and the PBS. Then,

we provide SAM and PBS results for the number of received molecules (NRM) which is proportional to CGF in two scenarios of single-object and double-objects in the diffusion environment. Finally, we provide bit error rate results for a simple on-off keying modulation scheme between elliptical transmitter and receiver.

A. Implementation of SAM and PBS

SAM: We elaborate the SAM implementation for a simple scenario where one elliptical object is located at the origin and the point transmitter is located at \bar{r}_{tx} . When there are multiple objects, the approach is similarly extended. As discussed in Section IV, given the point source at \bar{r}_{tx} , CGF $G(\bar{r}', \omega | \bar{r}_{tx}, t_0)$ at an arbitrary point \bar{r}' is computed by (32) by having $G(\bar{r}, \omega | \bar{r}_{tx}, t_0)$ and $\nabla G(\bar{r}, \omega | \bar{r}_{tx}, t_0)$ for the boundary points $\bar{r} \in \partial\mathcal{D}$. $G(\bar{r}, \omega | \bar{r}_{tx}, t_0)$ and $\nabla G(\bar{r}, \omega | \bar{r}_0, t_0)$ are expanded in terms of pulse basis functions over the boundaries. To obtain the unknown coefficients for these functions, the integral equation of (32) needs to be solved for some observation points on the boundaries. This leads to the matrix equation of (55) from which the vector of unknown coefficients is computed.

To this end, the object boundary is meshed and the DCM matrix is characterized. Corresponding each m th mesh, one matching point (observation point) is considered whose location (x_m, y_m) represents the midpoint of the m th mesh. For the current 2D problem, the surface integral of (53) reduces to a line integral and the element of m th row and n th column of $[\tilde{K}]$ ($m \neq n$) is approximated by the rectangular rule as³

$$\begin{aligned} \tilde{K}t_{mn} \approx & (\mathcal{L}(\omega)H(x_m, y_m | x_n, y_n) - DH_x(x_m, y_m | x_n, y_n)n_x \\ & - DH_y(x_m, y_m | x_n, y_n)n_y)l_n, \end{aligned} \quad (59)$$

where l_n is the length of n th mesh and

$$H(x_m, y_m | x_n, y_n) = \frac{-j}{4D} \mathcal{H}_0^{(2)}(Qd_{mn}), \quad (60)$$

$$\begin{aligned} H_x(x_m, y_m | x_n, y_n) &= \frac{\partial H(x, y | x_n, y_n)}{\partial x} \Big|_{x_m, y_m} \\ &= \frac{-j}{4D} \frac{x_m - x_n}{d_{mn}} \times \mathcal{H}_1^{(2)}(Qd_{mn}), \end{aligned} \quad (61)$$

$$H_y(x_m, y_m | x_n, y_n) = \frac{-j}{4D} \frac{y_m - y_n}{d_{mn}} \times \mathcal{H}_1^{(2)}(Qd_{mn}), \quad (62)$$

where $d_{mn} = \sqrt{(x_m - x_n)^2 + (y_m - y_n)^2}$. Considering the obstacle whose center is located at the origin, the normal vector at the boundary point (x, y) is given by

$$\hat{n} = n_x \hat{x} + n_y \hat{y} = \frac{-x}{a^2 \sqrt{\frac{x^2}{a^4} + \frac{y^2}{b^4}}} \hat{x} + \frac{-y}{b^2 \sqrt{\frac{x^2}{a^4} + \frac{y^2}{b^4}}} \hat{y}, \quad (63)$$

³The approximation approaches exact value for enough large number of meshes.

where \hat{x} and \hat{y} are unit vectors of coordinate system.

For ($m = n$) the Hankel function in (62) is singular and we insert the small argument approximation of zero and first order Hankel function to the line integral of (53) and perform the integral analytically, which yields

$$[\tilde{K}]_{mm} = \frac{-j}{4D} l_m \times (1 - 2j/\pi \log(0.164Ql_m)) - \frac{jQ^2(l_m^2)}{96} - \frac{j l_m}{\pi}. \quad (64)$$

Having DCM, $[U]$ is obtained from (55). By having $[U]$, time domain CGF could be computed by taking inverse Fourier transform from $G(\bar{r}', \omega, \bar{r}_0)$ given by (32), for arbitrary observation point \bar{r}' .

We note the frequency steps and the maximum frequency to implement the proposed SAM in a convergent manner is adopted $\Delta\omega = 0.01$ Hz and $\omega_{max} = 1000$ Hz, respectively.

PBS: To confirm the proposed approach, a particle based simulator (PBS) is implemented in MATLAB. In the PBS, time is divided into time steps of Δt s (seconds). In each time step, the information molecule locations are updated following random Brownian motion. The molecules move independently in the 2D space. The displacement of a molecule in each dimension over Δt s is modeled as a Gaussian random variable (RV) with zero mean and variance $2D\Delta t$. Considering the degradation reaction given in (4), a molecule may be removed from the environment during a time step Δt s, with probability $1 - \exp(-k_d\Delta t)$ [43] that is approximated with $k_d\Delta t$ for sufficiently small values of $k_d\Delta t$. Based on (58), if a molecule hits the boundary, the molecule may bind with receptor type- R_u and produce complex type- AR_u with probability $k_f^u \sqrt{\frac{\pi\Delta t}{D}}$. We note that employing this probability for simulating the boundary condition results in quantitatively accurate PBS, when the simulation time steps or adsorption coefficients are very small or the modeled system is kept well mixed [44]. Each bound molecule has the chance to unbind and return to the environment with probability $1 - e^{-k_b^u\Delta t}$ or may be internalized to the boundary with probability of $1 - e^{-k_v^u\Delta t}$ or remain in bound form. The number of molecules released by the transmitter to perform the PBS (the number of realizations) is $N_A \in \{2 \times 10^6, 10^7\}$ molecules.

B. Single-object scenario

We assume a single object in the environment whose center is located at the origin and the point transmitter at $\bar{r}_{tx} = (-5, 0)$ μm . In order to evaluate the convergence of the SAM in terms of number of meshes, we define an error function as follows

$$\text{Er}(M) = \frac{\| \int_0^{\omega_{max}} ([U]_M - [U]_{M-1}) d\omega \|}{\| \int_0^{\omega_{max}} [U]_{M-1} d\omega \|}, \quad (65)$$

where $[U]_M$ and $[U]_{M-1}$ denote $[U]$ obtained based on meshing the object boundary with M and $M - 1$ meshes, respectively, and $\| \cdot \|$ is the euclidean norm. Fig. 3 illustrates $\text{Er}(M)$ for circular object with different radius values a_o , when $k_f^o = 10^{-4} \text{ m s}^{-1}$, $k_b^o = 20 \text{ s}^{-1}$, and $k_v^o = 20 \text{ s}^{-1}$. The method is convergent with error ϵ , when there exist a number of meshes \mathcal{M} such that $\text{Er}(M) < \epsilon$ for all $M \geq \mathcal{M}$. For example,

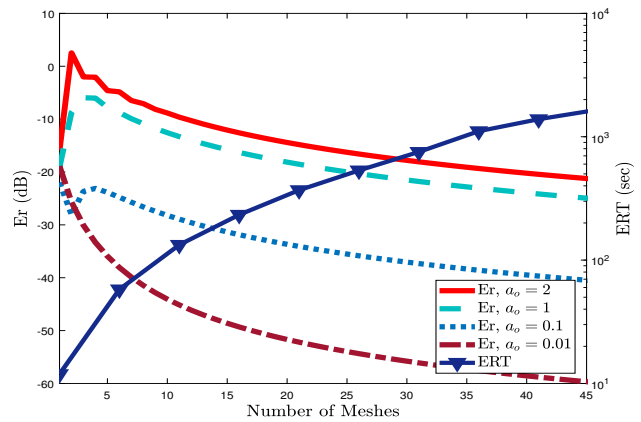


Fig. 3. Convergence error (Er) and expected run time (ERT) versus number of meshes for different obstacle radius.

we observe the convergence with error -10 dB occurs for $M \geq 10$ for all for a_o values. As shown, the convergence of the proposed SAM is fulfilled for the smaller number of meshes, when the obstacle radius decreases.

Fig. 3 also includes the expected run time (ERT) versus the number of meshes which is the same for different radius values. It is observed that the ERT behavior is exponentially increasing versus the number of meshes. However, it is still very fast (around 100 s) even for the number of meshes around 10. As mentioned before, the SAM is significantly less complicated compared to the simulation-driven approaches that mesh the n-dimensional diffusion space, since it requires meshing the boundaries utilizing the analytical CLIE. SAM method is even expected to be faster than the simulation-driven approaches that use the discretized time and continuous space as the most common simulation method within the MC research community. For instance, the expected run time for the PBS in the same computer in time interval $[0, 0.15]$ s for the same scenario is 2593 s and 12740 s when the number of realizations are 2×10^6 and 10^7 , respectively. The run times are the same for different radius values. This is much larger than the ERT for SAM which is around 100 s for 10 meshes which gives the CGF in the time interval $[0, 200]$ s.

Fig. 4 shows the NRM by a transparent receiver at $(5, 0)$ μm obtained from the SAM and PBS when the obstacle is located at $(0, 0)$ and the point transmitter is located at $\bar{r}_{tx} = (-5, 0)$ μm in a diffusive environment with $k_d = 20$. The figure includes the SAM as well as PBS results for partially absorbing obstacle ($k_f^o = 10^{-4} \text{ m s}^{-1}$, $k_b^o = 20 \text{ s}^{-1}$, $k_v^o = 30 \text{ s}^{-1}$), fully-absorbing ($k_f^o = \infty$) and fully-reflective ($k_f^o = 0$) boundary conditions when $(a_o, b_o) \in \{(2, 1) \mu\text{m}, (1, 1) \mu\text{m}\}$. As expected, increasing k_f^o at the obstacle leads to absorption of more molecules by the obstacle which degrades the NRM at the receiver. Further, Fig. 4 enables capturing the effect of the obstacle shape on NRM. Changing the shape of the obstacle from elliptic to circle amplifies the NRM as expected. Also, we observe that the degree of absorption at the obstacle (different values of k_f^o) does not change the peak time while the peak value changes

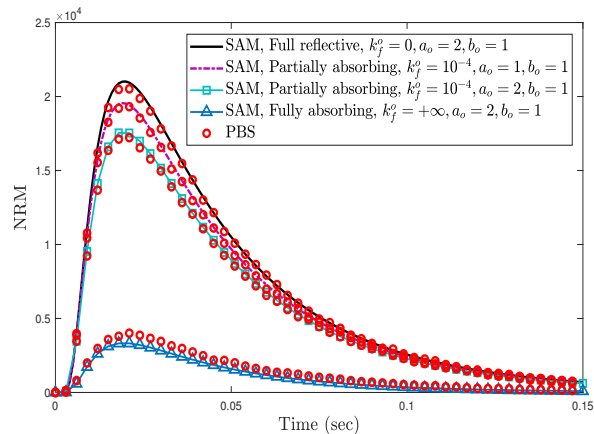


Fig. 4. NRM at transparent receiver obtained from SAM and PBS when one obstacle is in the diffusion environment with different boundary conditions and geometries.

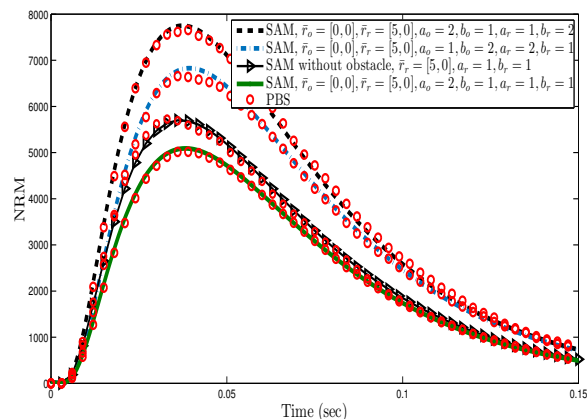


Fig. 5. NRM at elliptic receiver obtained from SAM and PBS in the presence (absence) of the elliptic obstacle for diffusion locations and geometries of objects.

significantly. We observe that the SAM result for the special case of fully-absorbing boundary, $k_f = \infty$, has a minor deviation from the PBS peak compared to the full match in other cases. This slight deviation may arise from the approximations in the numerical computations for the special case of $k_f = \infty$, e.g., computation of the self terms in the DCM and the choice of basis functions.

C. Double-object scenario

In this subsection, we assume there are two elliptic objects in the environment. First, consider one of the objects is the receiver and the other one is the obstacle. The receiver is located at \bar{r}_r with a_r, b_r , and $k_f^r = 10^{-4} \text{ m s}^{-1}, k_b^r = 20 \text{ s}^{-1}, k_f^o = 20 \text{ s}^{-1}$, when the fully-reflective obstacle is located at \bar{r}_o with a_o, b_o , and the transmitter is located at $\bar{r}_{tx} = (-5, 0) \mu\text{m}$. Fig. 5 illustrates the number of received AR_r molecules at the receiver for different locations and geometries of the receiver and obstacle. For comparison, the result for the scenario without the obstacle has also been

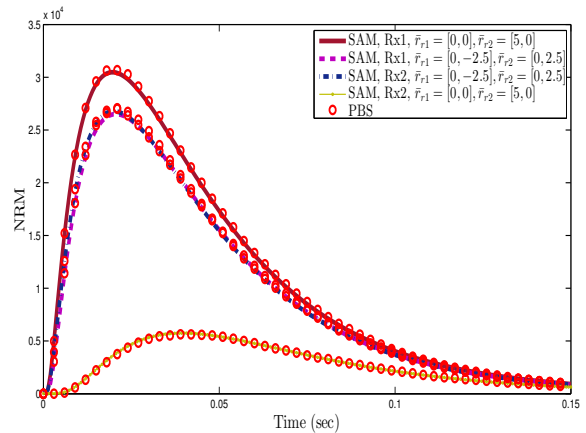


Fig. 6. NRM obtained from SAM and PBS at two elliptic receivers located at diffusion locations and with different geometries.

presented in this figure. We observe that PBS confirms SAM results. The NRM obtained from SAM captures the effect of the obstacle and see that the NRM weakens in the presence of obstacle. Also, comparing the results in this figure for different axes lengths of elliptical receiver and obstacle, reveals the sensible affect on the NRM.

In Fig. 6, we have assumed two objects in the environment as elliptic receivers with $(a_{r1}, b_{r1}) = (1, 2) \mu\text{m}$, $(a_{r2}, b_{r2}) = (2, 1) \mu\text{m}$, $k_f^{r1} = k_f^{r2} = 10^{-4} \text{ m s}^{-1}, k_b^{r1} = k_b^{r2} = 20 \text{ s}^{-1}, k_f^o = k_v^o = 20 \text{ s}^{-1}$, when $k_f = 10^{-4} \text{ s}^{-1}$ and $k_b = 20 \text{ s}^{-1}$ are considered for both receivers. This figure depicts the NRM at the receivers whose centers are located at two different configurations. In the vertical configuration, the receivers are located at $\bar{r}_{r1} = [0, -2.5] \mu\text{m}$ and $\bar{r}_{r2} = [0, 2.5] \mu\text{m}$ and in the horizontal configuration they are at $\bar{r}_{r1} = [0, 0] \mu\text{m}$ and $\bar{r}_{r2} = [5, 0] \mu\text{m}$. As observed, PBS follows accurately SAM results when there are also two partially absorbing receivers in the environment. As expected, it is observed that for vertical configuration, the NRM at both receivers coincides. As observed, PBS follows accurately SAM results when there are also two partially absorbing receivers in the environment. As expected, it is observed that for vertical configuration, the NRM at both receivers coincides.

D. Bit error rate

In this subsection, the average received signal at the receiver obtained from SAM is used to compute the error probability of diffusive molecular communication system between two elliptic receiver and transmitter.

The transmitter is assumed to be an ellipse located at $\bar{r}_t = (0, 0)$ with $(a_t, b_t) = (2, 1) \mu\text{m}$ that releases molecules uniformly over its boundary. Also, the boundary of the transmitter reacts reflective against the molecules inside the environment. The receiver is also an ellipse located at \bar{r}_r with $(a_r, b_r) = (1, 2) \mu\text{m}$. A simple on-off keying modulation scheme is considered where 0 and 1 are represented by instantaneously releasing 0 and N_{tx} molecules (on average) by the transmitter, respectively. The receiver counts the number

of ligand-receptor complexes AR_r bounded over its surface at sampling time t_s which maximizes probability of observation of the complex AR_r by the receiver given the release of one molecule from the transmitter in each time slot. We note that a molecule released at any point over the transmitter boundary may be observed at any point over the receiver boundary. To derive the observation probability of a molecule at the receiver, we average over the concentration Green's function for ligand-receptor complexes given the release points over the transmitter boundary and also receiver boundary. Thereby, we obtain

$$p_{\text{obs}}(t) = \frac{\int_{\bar{r}_0 \in \partial \mathcal{D}_t} \int_{\bar{r} \in \partial \mathcal{D}_r} C_{AR_r}(\bar{r}, t | \bar{r}_{tx}, t_0) dl_r dl_t}{L_r L_t}, \quad (66)$$

where L_r and L_t are circumference of the elliptic receiver and transmitter, respectively, $C_{AR_r}(\bar{r}, t | \bar{r}_{tx}, t_0)$ denotes the concentration Green's function of AR_r complexes over the receiver boundary point \bar{r} given the point transmitter at \bar{r}_{tx} which is provided as the Fourier inverse of (43). The receiver decides about the transmitted bit based on the observed sample.

In each time slot $t \in [0, T_0]$, the release rate of molecules can be modeled as a Poisson process [36] of $\text{Poisson}(s(t))$ given the average modulated signal $s(t)$. Thus, the number of the molecules observed at the receiver at time $t \in [0, T_0]$, i.e. $\mathbf{y}(t)$, from the released molecules at this time slot follows the Poisson process of $\mathbf{y}(t) \sim \text{Poisson}(s(t) \otimes p_{\text{obs}}(t))$ where \otimes denotes the convolution operator.

We employ a genie-aided decision feedback (DF) detector in which a genie informs the detector of the previously transmitted bits. Given the correct values of the previously transmitted bits and equal probability of bits 0 and 1, the Maximum-A-Posteriori (MAP) detector for a bit leads to a threshold decision rule. Derivation of corresponding BER is given in our previous works [21], [24].

Fig. 7 depicts the BER analysis versus time-slot duration for different reception mechanisms (boundary conditions) at the receiver $k_f^r \in \{10^{-4}, \text{and } +\infty\} \text{ m s}^{-1}$ and different degradation constants $k_d \in \{0, 20\} \text{ s}^{-1}$ when $k_b^r = 20 \text{ s}^{-1}$, $k_v^r = 20 \text{ s}^{-1}$, $k_f^t = 0$, $\bar{r}_t = (0, 0)$, $\bar{r}_r = (0, 10) \mu\text{m}$. As expected, increasing k_f^r , the NMR received at the surface of the receiver increases which results in decreased BER. Also, lower k_d leads to a higher channel memory and then higher inter-symbol interference in one hand, and in other hand, it increases the channel gain. We observe that for this scenario, the channel gain is dominant and decrease of k_d from 20 to 0 leads to lower error probability. Fig. 8 demonstrates the BER versus time-slot duration for different distances between transmitter and receiver of $\{5, 7, 10\} \mu\text{m}$ when $k_d = 20 \text{ s}^{-1}$, $k_f^r = 10^{-4} \text{ m s}^{-1}$, $k_b^r = 20 \text{ s}^{-1}$, $k_v^r = 20 \text{ s}^{-1}$, $k_f^t = 0$, and $\bar{r}_t = (0, 0)$. As expected, the performance of the DMC system significantly degrades by increasing the distance between transmitter and receiver.

VI. CONCLUSION

In this paper, we proposed a semi-analytic method (SAM) to obtain the fundamental concentration Green's function (CGF)

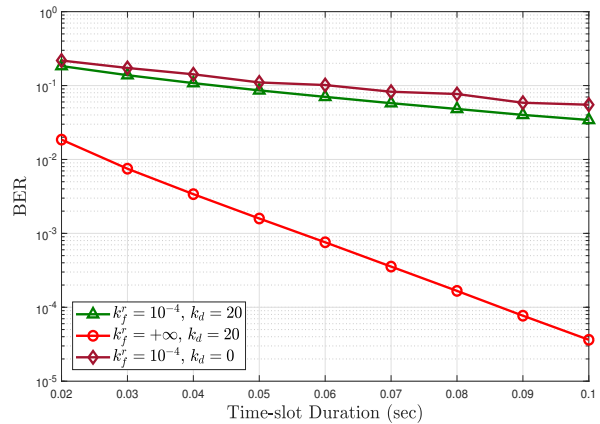


Fig. 7. Error probability for different boundary conditions at the receiver.

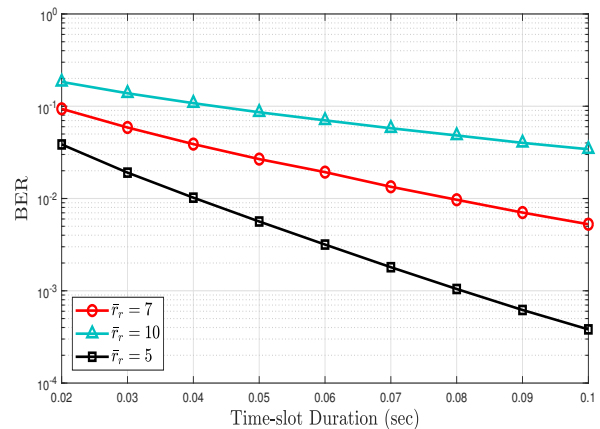


Fig. 8. Error probability for different distances between the transmitter and the receiver.

to model communication channels in the diffusive molecular communication networks (DMCN) with multiple transmitters, receivers, or other objects with arbitrary geometries and homogeneous boundary conditions. This method is significantly less complex compared to the pure simulation approaches and has higher flexibility for using in a wide range of geometries and boundary conditions compared to the pure analytical approaches. The proposed SAM relates the CGF at an arbitrary point to the CGF values over the boundaries and the known CGF for the unbounded environment through the concentration Green's function linear integral equation (CLIE). Using the method of moments, obtaining the unknown CGF values over the boundaries is reduced to the inverse of diffusion characteristic matrix (DCM). The DCM elements are functions of Green's function for unbounded environment and the geometry of the environment, independent of the source location and observation point. Further, we proposed the sequential SAM which includes boundaries to the environment sequentially. Thereby, the overall computational complexity decreases by transforming the inverse of a large matrix to the inverse of multiple smaller matrices. Also, the sequential SAM method

enables us to reuse the Green's function of the environment when a new object e.g., transmitter, receiver, or obstacle is added to the environment. Provision of a simulator based on the proposed method seems emergent for the area of molecular communication which is left for the future.

VII. ACKNOWLEDGMENT

This work was supported in part by European Research Consortium for Informatics and Mathematics (ERCIM) through postdoc fellowship awarded to Dr. Hamidreza Arjmandi and the Research Council of Norway (RCN:CIRCLE—Communication Theoretical Foundation of Wireless Nanonetworks) under Grant #287112.

REFERENCES

- [1] T. Nakano, A. W. Eckford, and T. Haraguchi, *Molecular Communication*, Cambridge, U.K.: Cambridge University Press, 2013.
- [2] I. F. Akyildiz, F. Brunetti, and C. Blázquez, "Nanonetworks: A new communication paradigm," *Computer Networks*, vol. 52, no. 12, pp. 2260-2279, Aug. 2008.
- [3] N. Farsad, H. B. Yilmaz, A. Eckford, C. B. Chae, and W. Guo, "A comprehensive survey of recent advancements in molecular communication," *IEEE Communications Surveys and Tutorials*, vol. 18, no. 3, pp. 1887-1919, Feb. 2016.
- [4] M. Pierobon and I. Akyildiz, "A physical end-to-end model for molecular communications in nanonetwork," *IEEE Journal on Selected Areas in Communications*, vol. 28, no. 4, pp. 602-611, May 2010.
- [5] M. S. Kuran, H. B. Yilmaz, T. Tugcu, and B. Özerman, "Energy model for communication via diffusion in nanonetworks," *Nano Communication Networks*, vol. 1, no. 2, pp. 86-95, Jun. 2010.
- [6] V. Jamali, A. Ahmadzadeh, W. Wicke, A. Noel, R. Schober, "Channel modeling for diffusive molecular communication—a tutorial review," *Proceedings of the IEEE*, vol. 107, no. 7, pp. 1256-1301, Jun. 2019.
- [7] M. Pierobon and I. F. Akyildiz, "A statistical physical model of interference in diffusion-based molecular nanonetworks," *IEEE Transactions on Communications*, vol. 62, no. 6, pp. 2085-2095, Jun. 2014.
- [8] M. H. Bazargani and D. Arifler, "Deterministic model for pulse amplification in diffusion-based molecular communication," *IEEE Communications Letters*, vol. 18, no. 11, pp. 1891-1894, Nov. 2014.
- [9] A. Noel, K. Cheung, and R. Schober, "Optimal receiver design for diffusive molecular communication with flow and additive noise," *IEEE Transactions on NanoBioscience*, vol. 13, no. 3, pp. 350-362, Sep. 2014.
- [10] A. Ajiz and A. H. Aghvami, "Error performance of diffusion-based molecular communication using pulse-based modulation," *IEEE Transactions on NanoBioscience*, vol. 14, no. 1, pp. 146-151, Jan. 2015.
- [11] A. Ahmadzadeh, H. Arjmandi, A. Burkovski and R. Schober, "Comprehensive Reactive Receiver Modeling for Diffusive Molecular Communication Systems: Reversible Binding, Molecule Degradation, and Finite Number of Receptors," *IEEE Transactions on NanoBioscience*, vol. 15, no. 7, pp. 713-727, Oct. 2016.
- [12] D. Kilinc and O. B. Akan, "Receiver design for molecular communication," *IEEE Journal of Selected Areas in Communications*, vol. 31, no. 12, pp. 705-714, Dec. 2013.
- [13] X. Wang, M. D. Higgins, and M. S. Leeson, "Relay analysis in molecular communications with time-dependent concentration," *IEEE Communications Letters*, vol. 19, no. 11, pp. 1977-1980, Nov. 2015.
- [14] M. U. Mahfuz, D. Makrakis, and H. T. Mouftah, "A comprehensive study of sampling-based optimum signal detection in concentration-encoded molecular communication," *IEEE Transactions on NanoBioscience*, vol. 13, no. 3, pp. 208-222, Sep. 2014.
- [15] N. Farsad, A. W. Eckford, S. Hiyama, and Y. Moritani, "On-chip molecular communication: Analysis and design," *IEEE Transactions on NanoBioscience*, vol. 11, no. 3, pp. 304-314, Sep. 2012.
- [16] M. S. Kuran, H. B. Yilmaz, and T. Tugcu, "A tunnel-based approach for signal shaping in molecular communication," *IEEE International Conference on Communications Workshops*, pp. 776-781, Jun. 2013.
- [17] L. Felicetti, M. Femminella, and G. Reali, "Establishing digital molecular communications in blood vessels," *First IEEE International Black Sea Conference on Communications and Networking (BlackSeaCom)*, pp. 54-58, Jul. 2013.
- [18] M. Turan, M. S. Kuran, H. B. Yilmaz, H. B., I. Demirkol, T. Tugcu, "Channel model of molecular communication via diffusion in a vessel-like environment considering a partially covering receiver," *IEEE International Black Sea Conference on Communications and Networking (BlackSeaCom)*, Aug. 2018.
- [19] W. Wicke, T. Schwering, A. Ahmadzadeh, V. Jamali, A. Noel, and R. Schober, "Modeling duct flow for molecular communication," *IEEE Global Communications Conference (GLOBECOM)*, pp. 206-212, Abu Dhabi, United Arab Emirates, Dec. 2018.
- [20] F. Dinc, F., B. C. Akdeniz, A. E. Pusane, T. Tugcu, "A general analytical approximation to impulse response of 3-D microfluidic channels in molecular communication," *IEEE transactions on nanobioscience*, vol. 18, no. 3, pp. 396-403, Mar. 2019.
- [21] M. Zoofaghari and H. Arjmandi, "Diffusive Molecular Communication in Biological Cylindrical Environment," *IEEE Transactions on NanoBioscience*, vol. 18, no. 1, pp. 74-83, Jan. 2019.
- [22] M. M. Al-Zu'bi and A. S. Mohan, "Modeling of ligand-receptor protein interaction in biodegradable spherical bounded biological micro-environments," *IEEE Access*, vol. 6, 25007-25018, May 2018.
- [23] X. Bao, Y. Zhu and W. Zhang, "Channel characteristics for molecular communication via diffusion with a spherical boundary," *IEEE Wireless Communications Letters*, vol. 8, no. 3 pp. 957-960, Feb. 2019.
- [24] H. Arjmandi, M. Zoofaghari, and A. Noel, "Diffusive molecular communication in a biological spherical environment with partially absorbing boundary," *IEEE Transactions on Communications*, vol. 67, no. 10, pp. 6858-6867, Jul. 2019.
- [25] L. Felicetti, M. Femminella, and G. Reali, "Simulation of molecular signaling in blood vessels: Software design and application to atherogenesis," *Nano Communication Networks*, vol. 4, no. 3, pp. 98-119, Sep. 2013.
- [26] I. Llatser et al., "Exploring the physical channel of diffusion-based molecular communication by simulation," in *IEEE Global Communication Conference (GLOBECOM)*, pp. 1-5, Dec. 2011.
- [27] H. B. Yilmaz and C.-B. Chae, "Simulation study of molecular communication systems with an absorbing receiver: Modulation and ISI mitigation techniques," *Simulation Modeling Practice and Theory*, vol. 49, pp. 136-150, Dec. 2014.
- [28] A. Noel, K. C. Cheung, R. Schober, D. Makrakis and A. Hafid, "Simulating with AcCoRD: Actor-based communication via reaction-diffusion," *Nano Communication Networks*, vol. 11, pp. 44-75, Mar. 2017.
- [29] B. Krishnaswamy, C. M. Austin, J. P. Bardill, D. Russakow, G. L. Holst, B. K. Hammer, C. R. Forest, and R. Sivakumar, "Time-Elastic Communication: Bacterial Communication on a Microfluidic Chip," *IEEE Transactions Communications*, vol. 61, no. 12, pp. 5139-5151, Dec. 2013.
- [30] A. O. Bicen, C. M. Austin, I. F. Akyildiz, and C. R. Forest, "Efficient Sampling of Bacterial Signal Transduction for Detection of Pulse-Amplitude Modulated Molecular Signals," *IEEE Transactions on Biomedical Circuits Systems*, vol. 9, no. 4, pp. 505-517, Aug. 2015.
- [31] L. Felicetti, M. Femminella, G. Reali, P. Gresele, M. Malvestiti, and J. N. Daigle, "Modeling CD40-Based Molecular Communications in Blood Vessels," *IEEE Transactions on NanoBioscience*, vol. 13, no. 3, pp. 230-243, Sep. 2014.
- [32] N. Farsad, W. Guo, and A. W. Eckford, "Tabletop Molecular Communication: Text Messages Through Chemical Signals," *PLOS ONE*, vol. 8, no. 12, p. e82935, Dec. 2013.
- [33] S. Giannoukos, A. Marshall, S. Taylor, and J. Smith, "Molecular Communication over Gas Stream Channels Using Portable Mass Spectrometry," *J. American Society for Mass Spectrometry*, vol. 28, no. 11, pp. 2371-2383, Nov. 2017.
- [34] H. Arjmandi, A. Gohari, M. Nasiri-Kenari, and Farshid Bateni, "Diffusion based nanonetworking: A new modulation technique and performance analysis," *IEEE Communications Letters*, vol. 17, no. 4, pp. 645-648, Apr. 2013.
- [35] G. Aminian, H. Arjmandi, A. Gohari, M. Nasiri-Kenari, and U. Mitra, "Capacity of diffusion-based molecular communication networks over LTI-Poisson channels," *IEEE Transactions on Molecular, Biological and Multi-Scale Communications*, vol. 1, no. 2, pp. 188-201, Nov. 2015.
- [36] H. Arjmandi, A. Ahmadzadeh, R. Schober, and M. N. Kenari, "Ion channel based bio-synthetic modulator for diffusive molecular communication," *IEEE Transactions on Nanobioscience*, vol. 15, no. 5, pp. 418-432, Jul. 2016.
- [37] P. Grindrod, *The theory and applications of reaction-diffusion equations: patterns and waves*, Clarendon Press, 1996.
- [38] D. Mehta and A.B. Malik, "Signaling mechanisms regulating endothelial permeability," *Physiological reviews*, vol. 86, no. 1, pp. 279-367, Jan. 2006.

- [39] H. Arjmandi, M. Zoofaghari, S. V. Rouzegar, M. Veletić, and I. Balasingham. "On mathematical analysis of active drug transport coupled with flow-induced diffusion in blood vessels." *IEEE Transactions on NanoBiosciencext* vol. 20, no. 1, pp.105-115, Jan. 2021.
- [40] J. Crank, *The mathematics of diffusion*. Oxford university press, 1979.
- [41] M. N. Sadiku, *Numerical techniques in electromagnetics*. CRC press, 2000.
- [42] W. C. Gibson, *The method of moments in electromagnetics*. Chapman and Hall/CRC, 2007.
- [43] Y. Deng, A. Noel, M. Elakashlan, A. Nallanathan, and K. C. Cheung, "Modeling and simulation of molecular communication systems with a reversible adsorption receiver," *IEEE Transactions on Molecular, Biological and Multi-Scale Communications*, vol. 1, no. 4, pp.347-362, Dec. 2015.
- [44] S. S. Andrews, "Accurate particle-based simulation of adsorption, desorption and partial transmission," *Physical Biology*, vol. 6, no. 4, Nov. 2009.



applied electromagnetic and microwave imaging.

Mohammad Zoofaghari was born in Isfahan, Iran, in 1986. He received the B.S. and M.S. degrees in Electrical Engineering from the Isfahan University of Technology, Isfahan, Iran, in 2009 and 2011, respectively, and the Ph.D. degree from the Amirkabir University of Technology, Tehran, Iran, in 2017. He is currently an Assistant Professor with the Department of Electrical Engineering, Yazd University, Yazd, Iran. His current research interests include channel modeling and estimation in molecular communication using analytical and numerical methods,



as an Assistant Professor with the Department of Electrical Engineering, Yazd University, Yazd, Iran, since 2016. His main research interests include molecular communications and nano-bio communication networks.

Hamidreza Arjmandi received the Ph.D. degree in electrical engineering from the Sharif University of Technology, Tehran, Iran, in 2016, and an M.Sc. degree in electrical engineering majoring in communication systems from the University of Tehran, Tehran, in 2010. He was awarded Postdoctoral Fellowship from the European Research Consortium for Informatics and Mathematics hosted by the Department of Electronic Systems, Norwegian University of Science and Technology, Trondheim, Norway, from 2019 to 2021. Also, he has been serving



Ali Etemadi received the B.Sc. degree in electrical engineering from the University of Tabriz, Tabriz, Iran, in 2010 and the M.Sc. degree in electrical engineering majoring in communication systems from Tarbiat Modares University, Tehran, Iran, in 2012, where he is currently pursuing the Ph.D. degree with the School of Electrical and Computer Engineering. His main research interests are molecular communication, biological modeling, statistical signal processing, and 5G network planning.



Ilango Balasingham received M.Sc. and Ph.D. degrees from the Department of Electronic Systems, Norwegian University of Science and Technology (NTNU), Trondheim, both in signal processing. He is Head of Section for Medical ICT R&D and the Intervention Centre, Oslo University Hospital, and Professor of Medical Signal Processing and Communications at NTNU. For the academic year 2016/2017, he was Professor by courtesy at the Frontier Institute, Nagoya Institute of Technology in Japan. His research interests include super robust

short-range communications for both in-body and on-body sensors, body area sensor networks, and nanoscale communication networks. He has authored or co-authored over 270 journal and full conference papers, 7 book chapters, 42 abstracts, 6 patents, and 20 articles in the popular press. He has given 16 invited/ keynotes at international conferences. He is a Steering Committee Member of ACM NANOCOM, Area Editor of Elsevier Nano Communication Networks.